On the Analysis of Body Orientation for Indoor Positioning with BLE 5.1 Direction Finding

Fabio Mavilia, Paolo Barsocchi, Francesco Furfari, Davide La Rosa, Michele Girolami
Italian National Council of Research, ISTI-CNR, Pisa, Italy
Email: {name.surname}@isti.cnr.it

***Abstract*—The last decade showed a clear technological trend toward the adoption of heterogeneous source of information, combined with data-fusion strategies to increase the performance of indoor localization systems. In this respect, the adoption of short-range network protocols such as WiFi and Bluetooth represent a common approach. We investigate, in this work, the use of Bluetooth 5.1 Direction Finding specification to test an indoor localization system solely based on the estimated Angle of Arrival (AoA) between an anchor and a receiver. We first detail our experimental data collection campaign and the adopted hardware. Then, we study not only the accuracy of the estimated angles on two reference planes but also the localization error introduced with the proposed algorithm by varying the body orientation of the target user, namely North, South, West, Est. Experimental results in a real-world indoor environment show an average localization error of 2.08m with only 1 anchor node and 5° of AoA' error for all 28 monitored locations. We also identify regions in which the AoA estimation rapidly decreases, giving rise to the possibility of identifying the boundaries of the adopted technology.**

***Keywords*-Bluetooth 5.1, Angle of Arrival, Indoor Localization, Proximity, Human Posture**

I. Introduction

The available technologies for localizing and tracking users in indoor environments are rapidly increasing their accuracy and availability also with commercial devices. In the past 10 years, we observed an interesting technological and algorithm trend moving towards the adoption of heterogeneous data combined with fusion strategies to estimate the position of a target in indoor environments [1]. In this respect, the use of wireless technologies plays a crucial role. In particular, short-range wireless interfaces such as Bluetooth, WiFi and Ultra Wide Band are widely adopted. Recently, the Bluetooth Special Interest Group has delivered a new protocol specification named Direction Finding (DF) in extension to the Bluetooth Core Specification 5.1. Such a new feature enables Bluetooth-compliant receivers to estimate not only the Received Signal Strength of Bluetooth messages but also the Angle of Arrival (AoA) between an emitter and a receiver. Bluetooth devices supporting the DF specification are characterized by an array of antennas combined with a micro-controller estimating the AoA. In this work, we describe the performance of an indoor localization system based on AoA estimation on azimuth and elevation planes. We discuss our experimental scenario and we detail the data collection process achieved with BT 5.1 compliant hardware kit. In particular, we estimate the position of a Bluetooth tag held by a person standing in different positions in a wide indoor environment. The person changes the body orientation of 90°, so that to reproduce 4 different layouts. More specifically, we firstly analyze two orthogonal aspects: the error introduced by the hardware kit for estimating the angle and the localization error. We show the MAE (Mean absolute error) given by comparing the estimated and actual AoA on two planes and on 4 orientations. Secondly, we study the localization error obtained by comparing the real and actual tag's location. Concerning the error introduced during the angle estimation, we observe that the highest errors derive from locations with the maximum azimuth angle, i.e. -77°to 77°. Moreover, from our analysis, we clearly distinguish the impact of the 4 user's orientations to the overall angle estimation. Concerning the performance of our localization algorithm, we obtain an average error of $2.08m$, with small variations according to the orientation of the person. In particular, the North orientation results with $1.89m$, the East orientation $2.26m$, the West orientation with $1.99m$ and the South orientation results with $2.17m$. The remaining of this paper is organized as follows. Section II summarizes works based on AoA estimation, Section III details the adopted hardware and the environment. Section IV analyzes the AoA of 4 different orientations, Section V describes the implemented algorithm and the performance we obtained.

Corresponding author: D. La Rosa {davide.larosa@isti.cnr.it}

II. Related Work

Recent years have shown an increasing interest to design and evaluate various techniques and technologies enabling indoor localization in indoor environments. In this section, we focus on the AoA technique available with the Bluetooth 5.1 specification, namely Direction Finding. Interested readers, can refer to [1], for a discussion concerning the current research trends of indoor localization. Most of the BT5.1 solutions in literature are based on simulations and only few works test such technology with real-world experimental settings. In [2] authors present a scenario with 2 fixed receiver anchors, based on Software Defined Radios (SDR) reproducing the packets Constant Tone Extension (CTE). The authors found that as the frequency of the used channels increases, the AoA average absolute error decreases. In [3], authors present an hybrid solution, based on the SLWSTK6006A[1] kit. The kit uses both

[1]https://www.silabs.com/development-tools/wireless/efr32xg21-wireless-starter-kit

the AoA and the RSSI of the Bluetooth signal to evaluate the transmitter's location. The experiment, carried out in a real scenario of 25x15m laboratory with four receiving anchors, obtained an average sub-meter error of 70cm computed on 8 locations. Furthermore, authors in [4] test the BOOSTXL-AOA kit to estimate the AoA and positioning errors in both indoor and outdoor environments. Tests conducted in indoor environments are performed with two anchors in a room of 20x25m with several obstacles such as walls, desks, tables and standing light. The computed average angular error, for angles between 15° and 90°, is 1.83°. The positioning error, computed on a smaller 5x5 2m-spaced locations grid, is 36.5cm. The previously mentioned works do not study in depth the impact of body attenuation to the localization process. To the best of our knowledge, only works based on the Bluetooth 4.x technology evaluate the impact of body on the signal propagation [5], [6], [7]. Differently, the goal of this work is to describe the impact of 4 different body orientations on the estimation of the AoA with a BT5.1-compliant hardware kit and to measure the localization error with such different orientations. Table I summarizes a selection of recent works, reporting: i) the number of deployed anchor nodes, ii) if the work considers the user's orientation , iii) features of the environment, iv) the number of evaluation points, v) average AoA error and vi) the obtained localization error.

III. The Experimental Settings

We now describe the experimental settings of our data collection campaign. We first introduce the adopted hardware (see Section III-A) and then we detail the environment in which we perform the tests (see Section III-B).

A. The Bluetooth 5.1 Hardware

We adopt the XPLR-AOA kit produced by ublox, shown in Fig. 1 comprising anchors and tags. Anchors have the following dimension: 11.5x11.5cm provisioned with 5 C211 antennas. Anchors are also provisioned with a micro-controller, namely the NINA-B411[2] BLE module and an USB port for I/O operations. The C209 tags are also provisioned with the NINA-B406 BLE module, advertising EddyStone beacon messages on 3 Bluetooth channels (37, 38 and 39). Tags can be configured to modify the advertisement rate in the range 1 to 50Hz as well as the power of transmission in the range -40dBm to 8dBm. Antennas support the possibility of installing a custom

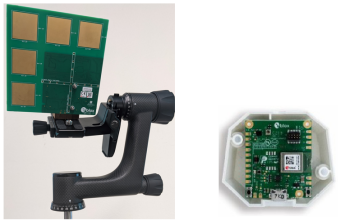

Fig. 1: The XPLR-AOA explorer kit: anchor and tag.

[2]https://www.u-blox.com/en/docs/UBX-20035327

firmware, in our case we upload the ublox firmware designed to log the following parameters:

- ϕ: the AoA between the tag and the azimuth plane (namely the XY plane), with the corresponding Received Signal Strength (RSS);
- δ: the AoA between the tag and the elevation plane (namely the plane orthogonal to the azimuth plane, passing through Z axis), with the corresponding RSS value;
- the advertisement channel used by the tag (37, 38, 39);
- the timestamp tracking the uptime of the logging node.

Data produced by the anchor are logged on the serial port with a frequency determined by the tag's advertisement frequency, which we set to 50Hz.

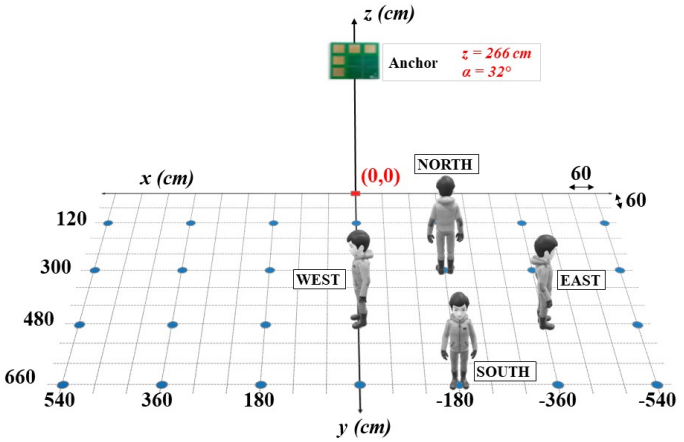

Fig. 2: The experimental environment: blue circles report the known locations, the anchor node is installed on the wall at $z = 266cm, \alpha = 32°$ inclination. Examples of the user orientations are reported on the map.

B. The Experimental Environment

Our testing environment is represented by a wide-empty room located in our research institute, ISTI-CNR in Italy. The room has the following dimension: 13.8x8m for a total area of about 110m^2 and 3.1m height. The floor is composed by regular tiles 60x60cm as depicted in Fig. 2. For the purpose of this experimental session, we use data collected from anchor A, deployed at $z = 266cm$ from the ground and with $\alpha = 32°$ inclination. This layout allows us to orientate the anchor toward the centre of the room. The tag is held on a lanyard. The position of the person varies among the 28 known locations (blue dots in Figure 2), where we collect 2 minutes of data from each of the locations. We then expect to collect at most 6000 samples from each of the 28 locations (we recall that we set to 50Hz the tag advertisement frequency). We also collect data by varying the orientation of the person. In particular, we perform 4 data collection campaigns in which the person is positioned 0°, 90°, 180°and 270°with respect to anchor A. From our experiments, we observe a wide range of angles both on the azimuth and elevation planes. More specifically, concerning the azimuth angle, we test the range: $-77° \leq \phi \leq 77°$, while for the elevation angle we test: $-20° \leq \delta \leq 19°$.

Work ref.	HW/SW	n° of anchors	Orientation	Environment[m]	eval. points	AoA mean error[°]	localization error[m]
[2]	SW (SDR)	2	✗	6x3	20	5	0.85
[3]	HW (SLWSTK6006A)	4	✗	25x15	8	?	0,7
[4]	HW (BOOSTXL-AOA)	2	✗	5x5	4	1.83	0.365
our work	HW (XPLR-AOA-1)	1	✓	13.8x8	28	5	2.08

TABLE I: Summary of BT5.1 experiments based on a real-world experimental setting.

IV. Analysis of AoA with Different Postures

We analyze the collected data from each of the 28 locations and from 4 different orientations, with the goal of assessing the errors introduced during the angle estimation for both azimuth and elevation. The following analysis allows us to exploit the angle estimation to implement and evaluate our indoor localization algorithm described in Section V. More specifically, we compute $\hat{\phi}$ and $\hat{\delta}$ for the 28 known locations, namely the angle's ground truth (GT), and we compare it against the estimated values ϕ and δ. The ground truth is obtained as follows. The GT azimuth angle is obtained as: $\phi = \arctan(x/y)$. Differently, the GT of the elevation angle between the anchor node and a tag at position (x, y) can be calculated as: $\delta(x, y, \alpha, A_z, T_z) = \beta - \theta$, with α tilt angle of the anchor's antenna, A_z height of the anchor and T_z height of the tag (as reported in Fig. 6):

$$\beta(x, y, \alpha) = \arccos\left(\frac{\sqrt{x^2 + y^2}}{\sqrt{x^2 + y^2 \cdot (1 + \tan^2(\alpha))}}\right) \quad (1)$$

and

$$\theta(x, y, A_z, T_z) = \arctan\left(\frac{A_z - T_z}{\sqrt{x^2 + y^2}}\right) \quad (2)$$

The comparison between real and estimated angled is computed with the MAE, mean absolute error metric, where n represents the number of collected samples for a given location ($n \leq 6000$):

$$MAE_\phi = \frac{\sum_{i=1}^{n} |\phi_i - \hat{\phi}_i|}{n}; MAE_\delta = \frac{\sum_{i=1}^{n} |\delta_i - \hat{\delta}_i|}{n} \quad (3)$$

Figures 3 and 4 report the contour maps showing the variation of the MAE on azimuth and elevation angles in 4 different orientations. The MAE is reported with a gradient colour, ranging from 0°to 50°. Concerning the azimuth plane (see Fig. 3), we observe that errors on the angle estimation are mainly generated on the corner locations, e.g. (-540,120), (540,120) or (540,680). Indeed, such locations represent the highest azimuth angle we can test with our experimental environment. Moreover, the orientation of the person holding the tag strongly influences the overall result. The North orientation provides the best performance, as the anchor node and the tag lie in the same line of sight. Conversely, the south orientation provides the worst results as the human body attenuates the signal propagation from the tag to the anchor node, resulting in remarkable errors. The East and West orientations provide intermediate results. In these two cases, we still observe higher errors in the corners of the experimental environment with respect to a central cone-shaped region where the angle estimation matches with the ground truth.

Concerning the elevation angle δ reported in Fig. 4, we still observe the same pattern of the azimuth plane. In particular, the North orientation provides the best performance, while the South orientation provides the worst accuracy. However, as a general trend, the MAE_δ is generally higher than MAE_ϕ, meaning that the elevation angle is estimated not as accurate as the azimuth angle. This consideration is particularly, evident with West and South orientations where the wide regions report high values of MAE_δ.

V. Detecting Human Indoor Positioning

We now detail our analysis concerning the performances of the algorithm. Section V-A describes the steps we follow to compute the position (x, y) of the tag in the map by processing both azimuth ϕ and elevation δ angles. Section V-B reports final results, showing how different orientations can affect the algorithm's performance.

A. The Indoor Localization Algorithm

In this section, we describe our localization algorithm designed to estimate the position of a tag by only using angles collected by the anchor node (see Section III), namely the azimuth ϕ and the elevation δ angles. The tag's position can be obtained by simply reversing the procedure used to calculate the angles' ground truth both for the azimuth and elevation angles. In particular, the coordinate x of the tag (see Fig. 5) is determined as the tangent of the azimuth angle, $x = y \cdot tan(\phi)$.

Differently, the y coordinate (see Fig. 6) is determined as the tangent of the angle $\theta = \beta - \delta$, where β is the angle of a point (x, y) on the anchor plane with α°inclination from the ceiling and δ is elevation angle:

$$y = \overline{\mathrm{AC}} = \frac{\overline{\mathrm{CT}}}{\tan(\theta)} = \frac{A_z - T_z}{\tan(\beta - \delta)} \quad (4)$$

where $(A_z - T_z)$ is the height difference between the anchor and the tag nodes. Equation (4) is valid only on plane $x = 0$, i.e. for the azimuth angles $\phi = 0$. In order to compute Equation 4 for any position (x, y), we transform $\beta(x, y, \alpha)$ defined in (2) to $\beta(\phi, \alpha)$ by using the relationship $x = \tan(\phi) \cdot y$:

$$\beta(\phi, \alpha) = \arccos\left(\frac{\sqrt{\tan^2(\phi) + 1}}{\sqrt{\tan^2(\phi) + 1 + \tan^2(\alpha)}}\right) \quad (5)$$

Considering equations (1) and (2), with the appropriate substitutions we now obtain:

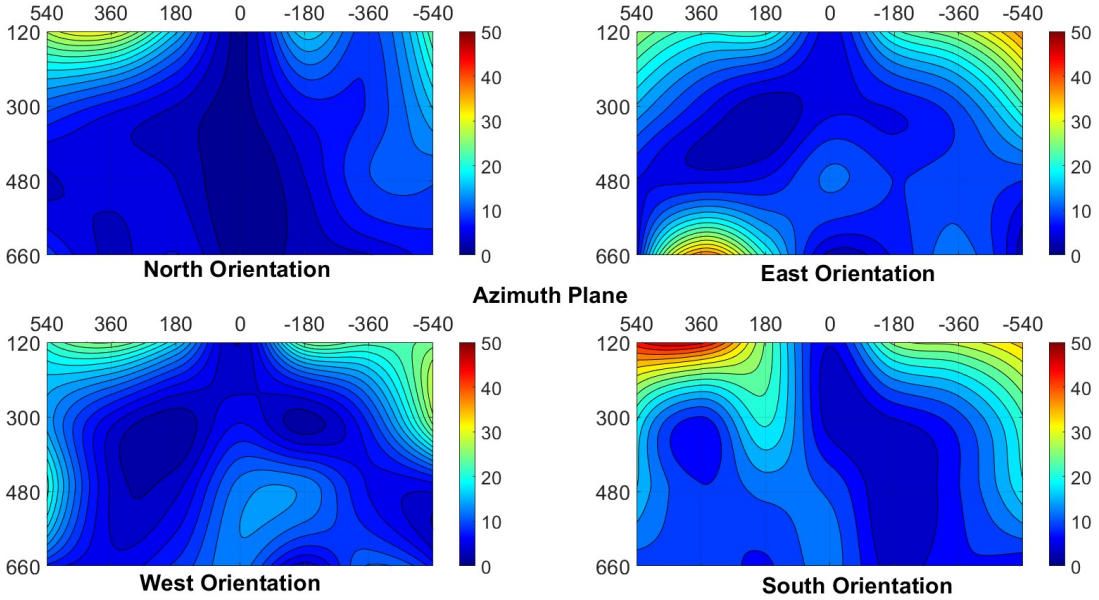

Fig. 3: MAE of azimuth angle ϕ (expressed in radius) relative to 4 orientations.

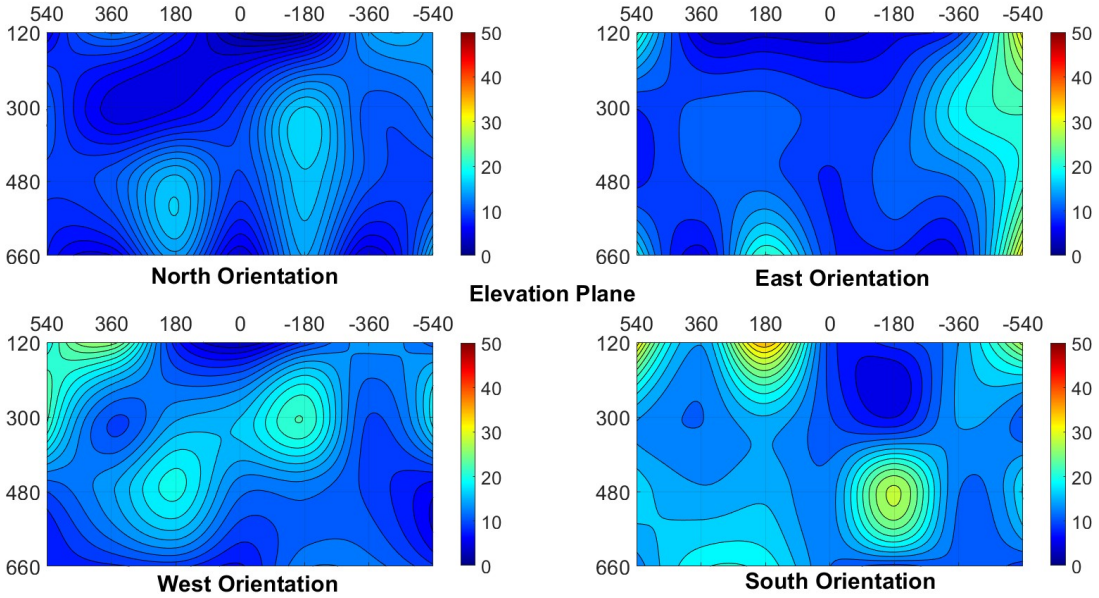

Fig. 4: MAE of elevation angle δ (expressed in radius) relative to 4 orientations.

$$x(\phi, \delta, A_z, T_z) = \tan(\phi) \cdot y \tag{6}$$

$$y(\phi, \delta, A_z, T_z) = \frac{A_z - T_z}{\tan(\beta(\phi, \alpha) - \delta) \cdot \sqrt{\tan^2(\phi) + 1}} \tag{7}$$

The denominator of Equation 4, namely $\tan(\theta)$, is zero for values of δ approaching to β and, consequently, the y coordinate tends also to infinity. From a geometrical perspective, this means that the measure of the elevation angle δ intrinsically leads to an error: the tag is considered at the same height as the anchor node and it is projected very far. Errors in the measurement of the elevation angle can be greatly amplified due to the tangent. In our setup, 1°error on the anchor tilt plane results with 3% relative error for y coordinate (about $12cm$ of absolute error), while 1° error measurement for elevations 30°above the tilt plane results with 33% relative error (about $19m$ of absolute error). In order to overcome such error, we apply a constraint discarding un-admissible angles. More specifically, we assume that δ is ignored according to

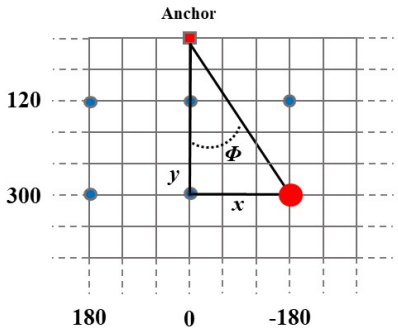

Fig. 5: Angle between the tag and the anchor on the azimuth plane.

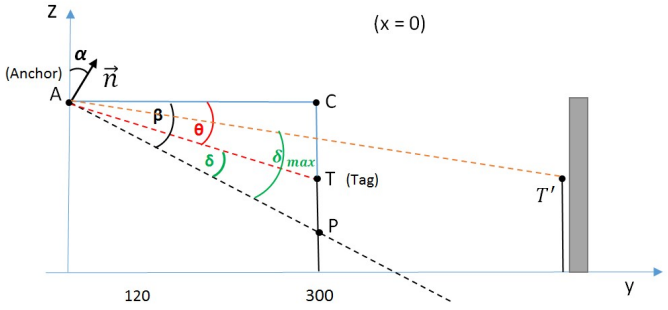

Fig. 6: Angle δ between the tag T and anchor A on the elevation plane ZY (x=0).

the following relationship:

$$\beta(\phi,\alpha) - \frac{\pi}{2} \geq \delta \geq \beta(\phi,\alpha)$$

As a practical example of the previously described constraint, we show in Fig. 6 a scenario in which tag T is positioned at the maximum distance from the anchor A. In this case, we calculate the maximum elevation angle δ_{max} between anchor and tag, δ_{max} represents our constraint that we consider to discard values of $\delta > \delta_{max}$.

B. Experimental Results

In this section, we report the results of the positioning algorithm previously described. As reported in Section IV, body's orientations influence the accuracy of the estimated azimuth and elevation angles. As a consequence, the resulting performances of the localization algorithm are also affected. Figure 7 reports the contour maps of the distances (expressed in meters) between the GT position of the tag and the algorithm's output in 4 orientations. The gradient colour ranges from 0 to 10 meters. We observe a close correlation between MAEs of both azimuth and elevation angles and the positions calculated by the algorithm. Indeed, in the regions where MAE_ϕ and MAE_δ are generally high, mostly on the corners, the positioning error is considerable.

We further present in Fig. 8 the distribution of distances for the 4 orientations as box plots with median (mid red line), $25th$ and $75th$ percentile, maximum and minimum. The goal is to show, quantitatively, how the distance error distributions are affected by human orientation. As a general trend, we can assert similar considerations concerning the AoA analysis. North orientation provides the best performance, with a median distance error of $1.81m$. Values range from a minimum of $0.04m$ in the point $(0, 120)$, up to $3.75m$ in the corner side. East and West orientations provide intermediate results, with a median value of $1.75m$ and $1.78m$, respectively. South orientation is the worst in terms of accuracy. Computed distances are generally higher than the other orientations caused by an evident effect of the body obstruction. Considering a real scenario where we cannot assume a priori the direction of a person in the environment, we combine the results of all the orientations, providing an overall performance assessment of the algorithm. Figure 9 shows the resulting contour map. Considering x-axis, the error increases proportionally to the distance of the tag from the anchor. More specifically, the error ranges from $0.04m$ ($x = 0$) up to $3.5m$ ($x = \pm 540$), approximately. On y-axis, the error trend is comparable up to about $y = 300$. Beyond this edge, in the central area of the room, the error ranges from 1.5 and 2.5 meters. As a general trend, the error increases with the distance from the anchor, reaching its maximum value on the room corners. As we report in Section V-A, applying the constraint $\delta > \delta_{max}$, the algorithm discards all the values which would position the person out of the room. The discard percentage is 44.6% on average for all the 4 orientations. As it is easy to imagine, on the extremities of the room, we register a very high percentage of discard caused by values of δ really close to δ_{max}. On the other hand, this percentage is generally low in the central area of the room, up to 0% close to the anchor.

VI. Conclusions

In this paper, we evaluated and discussed the use of Bluetooth 5.1 Direction Finding specification as the main technology to estimate a user's position in indoor environments. In particular, we first showed and commented on the mean absolute error between estimated and real angles on the two planes with 4 different user's orientations. From our analysis, we clearly distinguish the impact of the 4 user's orientations to the overall angle estimation. When the user is in front of the anchors (North orientation), the estimated azimuth angle is near to the actual value. However, even in the other orientations, we observe that in centred positions the error is small, while errors increase in the peripheral locations. Indeed, such locations represent the highest azimuth angle that we can test with our experimental hardware. Conversely, the South orientation provides the worst results, as the human body attenuates the signal propagation from the tag to the anchor node, resulting with remarkable errors. The East and West orientations provide intermediate results. In these two cases, we still observe higher errors in the corners of the experimental environment with respect to a central cone-shaped region where the angle estimation matches the ground truth. Secondly, we studied the localization errors obtained by comparing the real position of

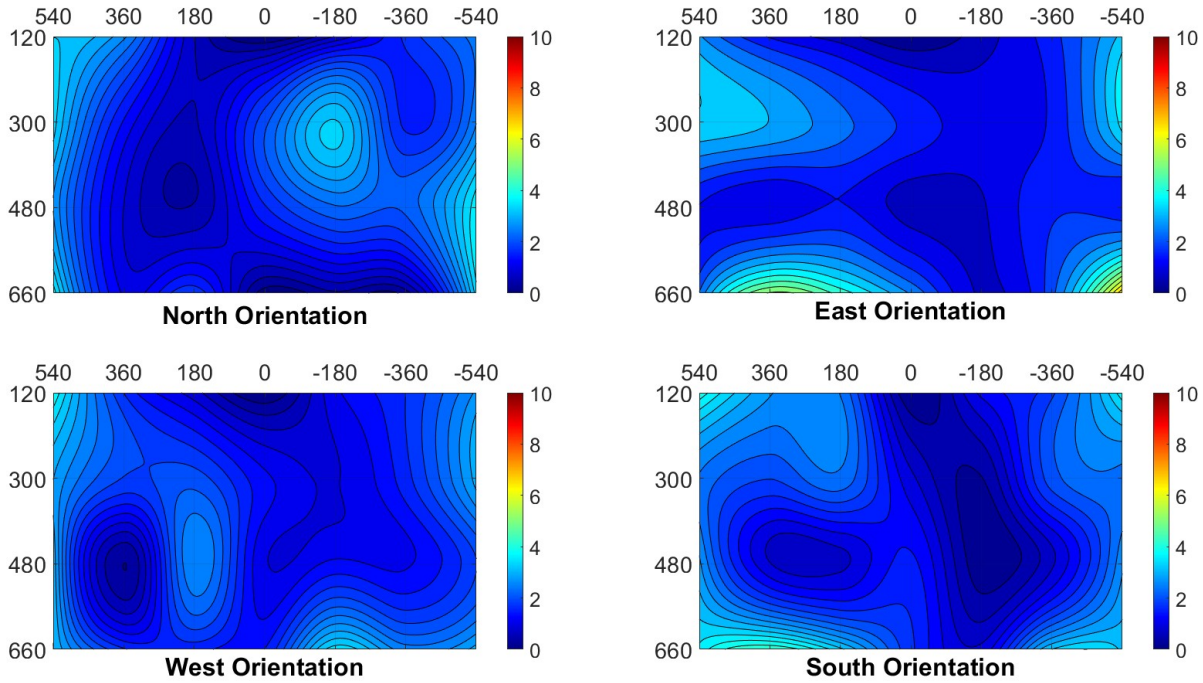

Fig. 7: Localization error expressed in meters between the GT position of the tag and the algorithm's output.

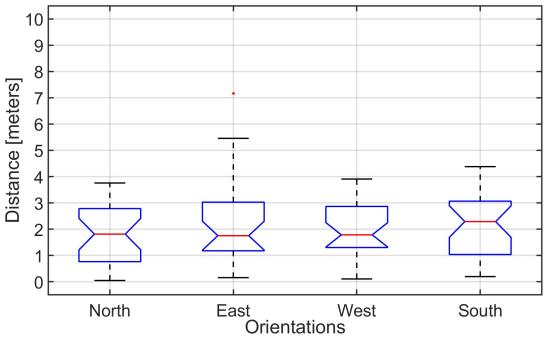

Fig. 8: Distribution of the localization error for different orientations.

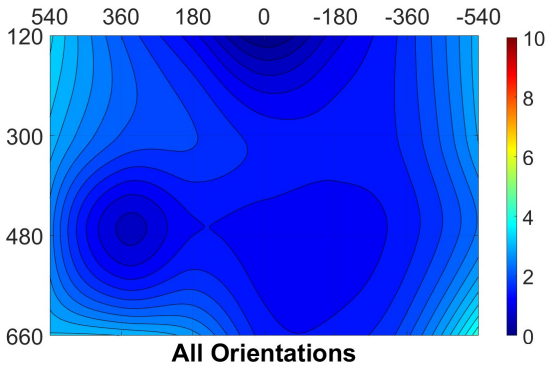

Fig. 9: Aggregation of the localization error expressed in meters for different orientations.

the tag compared to the estimated position resulting from our localization algorithm. We observe that by only deploying one anchor node in the monitored environment, the localization errors are constrained in a range of $[0 - 5m]$. Further lines of investigation include the joint use of RSSI and AoA estimation and the use of multiple anchor nodes to further reduce the localization error.

Acknowledgment

This work is partially supported by the ChAALenge project (B89J22002310005) and PNRR-PE8 AGE-IT project (B83C22004880006).

References

[1] F. Potortì, A. Crivello, F. Palumbo, M. Girolami, and P. Barsocchi, "Trends in smartphone-based indoor localisation," in *2021 International Conference on Indoor Positioning and Indoor Navigation (IPIN)*. IEEE, 2021, pp. 1–7.

[2] M. Cominelli, P. Patras, and F. Gringoli, "Dead on arrival: An empirical study of the bluetooth 5.1 positioning system," in *Proceedings of the 13th International Workshop on Wireless Network Testbeds, Experimental Evaluation and Characterization*, ser. WiNTECH '19. New York, NY, USA: Association for Computing Machinery, 2019, p. 13–20.

[3] G. Pau, F. Arena, Y. E. Gebremariam, and I. You, "Bluetooth 5.1: An analysis of direction finding capability for high-precision location services," *Sensors*, vol. 21, no. 11, 2021.

[4] P. Sambu and M. Won, "An experimental study on direction finding of bluetooth 5.1: Indoor vs outdoor," in *IEEE Wireless Communications and Networking Conference*, 2022, pp. 1934–1939.

[5] P. Baronti, M. Girolami, F. Mavilia, F. Palumbo, and G. Luisetto, "On the analysis of human posture for detecting social interactions with wearable devices," in *2020 IEEE International Conference on Human-Machine Systems (ICHMS)*, 2020, pp. 1–6.

[6] M. J. Christoe, J. Yuan, A. Michael, and K. Kalantar-Zadeh, "Bluetooth signal attenuation analysis in human body tissue analogues," *IEEE Access*, vol. 9, pp. 85 144–85 150, 2021.

[7] M. Shi and L. Kreitzman, "Contact tracing for covid-19 using bluetooth low energy," *Journal of Student Research*, vol. 11, no. 1, Feb. 2022.